

Closed-form solutions for the inverse kinematics of serial robots using conformal geometric algebra

Isiah Zaplana^{a,*}, Hugo Hadfield^b, Joan Lasenby^b

^a*Department of Mechanical Engineering, KU Leuven – University of Leuven, Leuven, Belgium*

^b*Department of Engineering, University of Cambridge, Cambridge, UK*

Abstract

This work addresses the inverse kinematics of serial robots using conformal geometric algebra. Classical approaches include either the use of homogeneous matrices, which entails high computational cost and execution time, or the development of particular geometric strategies that cannot be generalized to arbitrary serial robots. In this work, we present a compact, elegant and intuitive formulation of robot kinematics based on conformal geometric algebra that provides a suitable framework for the closed-form resolution of the inverse kinematic problem for manipulators with a spherical wrist. For serial robots of this kind, the inverse kinematics problem can be split in two subproblems: the position and orientation problems. The latter is solved by appropriately splitting the rotor that defines the target orientation in three simpler rotors, while the former is solved by developing a geometric strategy for each combination of prismatic and revolute joints that forms the position part of the robot. Finally, the inverse kinematics of 7 DoF redundant manipulators with a spherical wrist is solved by extending the geometric solutions obtained in the non-redundant case.

Keywords: serial robots, redundant robots, inverse kinematics, geometric algebra, conformal geometric algebra

1. Introduction

A serial robot is an open kinematic chain made up of rigid bodies, called *links*, connected by kinematic pairs, called *joints*, that provide relative motion between consecutive links. The point at the end of the last link is known as the *end-effector*. Only two types of joints are considered throughout this work: *revolute (prismatic)* joints, that perform a rotational (translational) motion around (along) a given axis.

*Corresponding author

Email addresses: isiah.zaplana@kuleuven.be (Isiah Zaplana), hh409@cam.ac.uk (Hugo Hadfield), j1221@cam.ac.uk (Joan Lasenby)

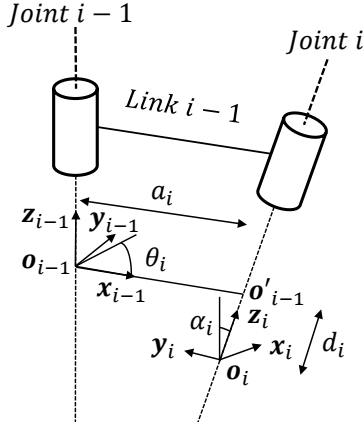


Figure 1: The four D-H parameters: the length of link i (a_i), the angle between the joint axes z_{i-1} and z_i (α_i), the distance between o_{i-1} and o_i along z_i (d_i) and the angle between x_{i-1} and x_i (θ_i). Clearly, if the $(i-1)$ -th and i -th joint axes intersect (are parallel), then $\alpha_i = 0$ ($\alpha_i = 0$) and d_i (a_i) is the length of the i -th link.

The end-effector position and orientation (also known as the *pose*) is expressed as a differentiable function $f : \mathcal{C} \rightarrow X$, where \mathcal{C} denotes the space of joint poses, known as the *configuration space* of the robot, while X denotes the space of all positions and orientations of the end-effector with respect to a reference frame, known as the *operational space* of the robot. We say that the *workspace* of the robot, denoted by \mathcal{W} , is the volume of the operational space X that is reachable by the robot's end-effector. We attach a frame to each joint of the robot so that it describes the relative position and orientation of the joint. The relations between consecutive joint frames can be expressed by homogeneous matrices based on the Denavit-Hartenberg convention [1]. This convention consists of the use of four parameters, the *D-H parameters* (figure 1): one acting as a *joint variable* – angle θ_i or displacement d_i , depending on the nature of the joint – and the other three acting as constants – length a_i , angle α_i and d_i or θ_i depending on which one describes the joint variable [2, 3]. In general, if the nature of the joint i is not specified, its joint variable is denoted by q_i . The vector of all joint variables is denoted by $\mathbf{q} = (q_1, \dots, q_n)$ and is known as the *configuration*. Therefore, the configuration space \mathcal{C} is the space of joint configurations. A robot is said to have n *degrees of freedom* (DoF) if its configuration can be minimally specified by n variables. For a serial robot, the number and nature of the joints determine the number of DoF. For the task of positioning and orientating its end-effector in the space, the manipulators with more than 6 DoF are called *redundant*, while the rest are *non-redundant*.

Therefore, we can associate a homogeneous matrix T_i^{i-1} with each joint frame $\{i\}$ such that it relates such frame to the preceding one, i.e., joint frame $\{i-1\}$. The first joint frame is related to the fixed reference frame. For each configuration $\mathbf{q} \in \mathcal{C}$, $f(\mathbf{q})$ can be represented using these homogeneous matrices

as follows:

$$T_n^0 = T_1^0 \cdot T_2^1 \cdot \dots \cdot T_n^{n-1} \quad (1)$$

with

$$T_n^0 = \begin{pmatrix} R & \mathbf{p} \\ 0 & 1 \end{pmatrix} \quad (2)$$

where R denotes the rotation matrix describing the end-effector orientation with respect to the fixed reference frame and \mathbf{p} is the vector that describes the end-effector position with respect to that reference frame [1, 2, 3]. An important class of serial robots are those with a spherical wrist. For these robots, the axes of their last three joints intersect at a common point, known as the *wrist center point*, or are parallel (the intersection point and, hence, the wrist center point, is the point at the infinity). In this context, the end-effector position, \mathbf{p} , can be moved to the wrist center point \mathbf{p}_w by a fixed translation and, thus, the last three joints would only contribute to the orientation of the end-effector.

This paper is focused on one of the most important problems in robot kinematics, namely the *inverse kinematic problem*. It consists of recovering the joint variables, i.e., the configuration, given a target end-effector pose. This configuration may not be unique, since non-redundant manipulators have up to sixteen different configurations for the same end-effector pose [4], while for redundant manipulators this number is unbounded [2, 3]. The opposite problem is known as the *forward kinematic problem* and consists of obtaining the pose of the end-effector given the value of the joint variables.

The inverse kinematic problem plays a major role in robotics, specially in robot kinematics, motion planning and control theory. There are different methods used to solve it and they are usually categorized in two groups:

- a) Closed-form methods: all the solutions are expressed in terms of the entries of 0T_n . These methods strongly depend on the geometry of the manipulator and, therefore, are not sufficiently general. However, it is clear that they have advantages over the numerical methods such as, for instance, lower computational cost and less execution time. Additionally, they give all the solutions for a given end-effector's pose. Some closed-form methods include strategies based on machine learning [5], matrix manipulations [4, 6], the definition of the arm angle parameter [7, 8] and different geometric methods [9, 10, 11].
- b) Numerical methods: a good approximation $\tilde{\mathbf{q}}$ of one of the solutions is derived iteratively. Although these methods usually work for any manipulator, they suffer from several drawbacks such as, for example, high computational cost and execution time, existence of local minima and numerical errors. Moreover, only one of the sixteen (infinite) possible solutions is obtained for non-redundant (redundant) manipulators. The most common numerical approaches are the Jacobian-based methods [12, 13, 14, 15, 16, 17].

Among all the methods presented in this section, the closed-form methods are the most suitable for serial robots since they allow us to obtain the set of all

solutions with a small computational cost. This paper proposes a formulation of the inverse kinematic problem based on conformal geometric algebra. This formulation allows us to avoid the use of matrices and, due to its inherent geometric nature, provides a geometrical description of the problem with which the inverse kinematics can be solved easily. These properties are exploited in this work to solve the inverse kinematics of serial robots with 6 DoF and spherical wrist. For these manipulators, this problem can be decoupled into two sub-problems: the position problem and the orientation problem. For the former, a classification of the different combinations of prismatic and revolute joints that describe the position part of the manipulator is made and a geometric strategy is developed to solve each one of them, while, for the latter, we split the rotor that defines the target orientation into three simpler rotors, each one of them depending on a unique joint variable. Finally, the inverse kinematics of redundant serial robots with 7 DoF and spherical wrist is solved by extending the geometric solutions obtained in the non-redundant case.

The rest of the paper is organized as follows: Section 2 reviews the related work and presents a basic introduction to geometric algebra. In Section 3, a description of the forward kinematics of an arbitrary serial robot based on conformal geometric algebra is given. The formulation of the inverse kinematic problem and its solution are developed in Sections 4 and 5. In Section 6, the inverse kinematics of 7 DoF redundant serial robots is solved by extending the strategies introduced in Section 6. Finally, Section 7 presents the conclusions.

2. Related work and mathematical preliminaries

2.1. Related work

As mentioned in the introduction, some closed-form methods are usually difficult to formulate and solve for non-redundant robots even if they have a spherical wrist. For instance, the Pieper method [4] allows us to obtain the solutions of the inverse kinematics as the solutions of a set of polynomials and, for a general serial robot with a spherical wrist, at least one of these polynomials is of degree four, which is, in general, difficult to solve.

On the other hand, the Paul method [6] consists of the manipulation of the homogeneous matrices of the relation (1) so the following family of matrix equations is obtained:

$$\left(T_{i-1}^{i-2}\right)^{-1} \cdots \left(T_1^0\right)^{-1} \cdot T_n^0 = T_i^{i-1} \cdots T_n^{n-1} \quad \text{for } i = 2, \dots, n. \quad (3)$$

The objective is to isolate those non-linear equations that contain just one joint variable. However, even if we find those equations, solving them analytically is, in general, difficult. Similarly, the formulation and implementation of geometric methods is also difficult. If, for instance, the circle intersection of a plane with a sphere is considered, then a system of two equations (one of them non-linear) must be solved. In this context, geometric algebra turns to be very useful. As stated in the introduction, geometric algebra and, in particular, the conformal

model of three-dimensional Euclidean space, provides a framework for modeling the kinematics and dynamics of rigid bodies that avoids the use of matrices. In addition, the geometric entities such as points, lines, planes or spheres can be represented with elements of the algebra.

Regarding the contributions using this framework, in [18, 19] analogous versions to the Paul and Pieper methods are presented. In both works, an easy and compact formulation of the problem is presented using the language provided by geometric algebra. However, they have the same drawbacks as the original methods. The approach presented in [20] develops a fast and heuristic method that solves the inverse kinematics of arbitrary redundant serial robots. Nevertheless, the orientation problem is not treated and, since it is a numerical method, only one solution is obtained. Similarly, the approach presented in [21] only solves the position problem for an anthropomorphic manipulator.

Other approaches are focused on the development of geometric strategies based on conformal geometric algebra for particular robots. For example, in [22], a kinematic model of a planar redundant manipulator is developed, while in [23] the inverse kinematics and the singularity problem are formulated and solved for a class of parallel robots. A 5 DoF serial robot is considered in [24], where the geometric strategy followed is the same as in [21]. There, different geometric objects are defined. These objects, as well as the relations between them, are described using conformal geometric algebra. The angles between such geometric entities correspond to the unknown joint variables. Finally, the approach developed in [25] solves the inverse kinematics of a 6 DoF humanoid leg. In [26], the authors solve geometrically the position problem of the 6 DoF Comau Smart-5 NJ-110, while in [27], particular solutions of the inverse kinematics of the UR5 and Agilus KR6 R900 are given. All of these works are based on the strategies introduced in [21, 24].

In this work, an approach to solve the inverse kinematics of arbitrary 6 and 7 DoF serial robots with a spherical wrist is presented. This approach is not focused on a particular robot but applies to an entire class of manipulators. Although not every single case is covered, the majority and most representative ones are treated in this work. This allows to illustrate the power of conformal geometric algebra when applied to the inverse kinematics of serial robots with spherical wrist as well as to provide a set of easy-to-implement geometric strategies which, in turn, is the main goal of the present work. In particular, the position problem is solved geometrically by extending the particular contributions of [21, 26, 28, 29, 30], while a novel method is developed for solving the orientation problem. This method involves splitting the rotor that defines the target orientation into three rotors, so that each one depends on just one joint variable. The main advantage of this strategy lies in the fact that this approach is still a closed-form method, i.e., all the solutions are obtained as analytical expressions in terms of the end-effector pose. In addition, we are dealing with arbitrary serial robots of 6 and 7 DoF, not just a particular robotic geometry. Finally, due to the simplicity of the problem formulation and the geometric nature of conformal geometric algebra, such expressions are obtained easily than with other closed-form approaches (such as, for instance, the ones reviewed here).

2.2. Mathematical preliminaries

Geometric algebra provides strong advantages with respect to more common approaches such as, for instance, that geometric objects and Euclidean transformations live in the same algebra, that the expressions from the algebra are coordinate free and that it is well adapted to deal with more general fields in science and engineering. In particular, it provides a compact and neat formulation of robot kinematics and its main problems. Throughout this section, a brief overview of both geometric algebra and conformal geometric algebra is presented. A more detailed treatment of the subject can be found in [31, 32, 33].

2.2.1. Geometric algebra

Let us consider the real vector space \mathbb{R}^n with orthonormal basis $\{e_1, \dots, e_n\}$. The geometric algebra of \mathbb{R}^n , denoted by \mathcal{G}_n , is a vector space where the operations defined in \mathbb{R}^n , i.e., the addition and multiplication by scalars, are extended naturally. An additional operation, the *geometric product*, is defined on the algebra \mathcal{G}_n and, acting on vectors is defined as:

$$\mathbf{v}_1 \mathbf{v}_2 = \mathbf{v}_1 \cdot \mathbf{v}_2 + \mathbf{v}_1 \wedge \mathbf{v}_2, \text{ for } \mathbf{v}_1, \mathbf{v}_2 \in \mathbb{R}^n, \quad (4)$$

where \cdot denotes the inner or dot product and \wedge denotes the outer product.

The outer product of two vectors $\mathbf{v}_1, \mathbf{v}_2$ is a new element of \mathcal{G}_n , which is termed a *bivector*, is said to have *grade* two and is denoted by $\mathbf{v}_1 \wedge \mathbf{v}_2$. By extension, the outer product of a bivector with a vector is known as a *trivector* and is denoted by $(\mathbf{v}_1 \wedge \mathbf{v}_2) \wedge \mathbf{v}_3$. Clearly, trivectors have grade three. This can be generalized to an arbitrary dimension. Thus,

$$(\mathbf{v}_1 \wedge \mathbf{v}_2 \wedge \dots \wedge \mathbf{v}_{r-1}) \wedge \mathbf{v}_r \quad (5)$$

denotes an *r-blade*, an element of \mathcal{G}_n with grade r .

A bivector $\mathbf{v}_1 \wedge \mathbf{v}_2$ can be interpreted as the oriented area defined by the vectors \mathbf{v}_1 and \mathbf{v}_2 . Thus, $\mathbf{v}_2 \wedge \mathbf{v}_1$ has opposite orientation and, from that, the anticommutativity of the outer product can be deduced. Analogously, a trivector is interpreted as the oriented volume defined by its three composing vectors. Since the volume generated by $(\mathbf{v}_1 \wedge \mathbf{v}_2) \wedge \mathbf{v}_3$ is the same as the volume generated by $\mathbf{v}_1 \wedge (\mathbf{v}_2 \wedge \mathbf{v}_3)$, it is also deduced that the outer product is associative. Therefore, *r-blades* can be denoted simply as:

$$\mathbf{v}_1 \wedge \mathbf{v}_2 \wedge \dots \wedge \mathbf{v}_r. \quad (6)$$

Linear combinations of *r-blades* are known as *r-vectors*, while linear combinations of *r-vectors*, for $0 \leq r \leq n$, are called *multivectors*.

Applied to the basis elements $\{e_i\}$, the geometric product acts as follows:

$$e_i e_j = \begin{cases} 1 & \text{for } i = j \\ e_i \wedge e_j & \text{for } i \neq j \end{cases} \quad (7)$$

Then, $\{e_1, \dots, e_n\}$ can be expanded to a basis of \mathcal{G}_n that contains, for each $0 \leq k \leq n$, $C(n, k)$ grade k elements:

$$\begin{aligned}
&\text{Scalar: } 1 \\
&\text{Vectors: } e_1, \dots, e_n \\
&\text{Bivectors: } \{e_i \wedge e_j\}_{1 \leq i < j \leq n} \\
&\text{Trivectors: } \{e_i \wedge e_j \wedge e_k\}_{1 \leq i < j < k \leq n} \\
&\vdots \\
&\text{n-blade: } e_1 \wedge \dots \wedge e_n
\end{aligned} \tag{8}$$

This allows to extend the geometric product defined in equation (4) to arbitrary multivectors. Readers interested in a detailed explanation of this extension are referred to [31]. The grade n element $e_1 \wedge \dots \wedge e_n$ is known as the *pseudoscalar* and is usually denoted by I_n . Pseudoscalars allow us to define one of the main operators of geometric algebra, the *dual operator*. Its action over an r -vector A_r is:

$$A_r^* = I_n A_r, \tag{9}$$

where A_r^* is an $(n - r)$ -vector. In particular, we have that for two multivectors A and B , the following identity holds:

$$(A \wedge B)^* = A \cdot B^*. \tag{10}$$

For \mathbb{R}^3 , the geometric algebra \mathcal{G}_3 has the following basis:

$$\{1, e_1, e_2, e_3, e_{12}, e_{13}, e_{23}, I_3\}, \tag{11}$$

where $e_{ij} = e_i \wedge e_j$.

In \mathcal{G}_3 , bivectors play an important role since they can be used to describe spatial rotations. Indeed, in geometric algebra, rotations are described using *rotors*. If a point $\mathbf{x} \in \mathbb{R}^3$ is rotated by an angle θ around an axis ℓ , the rotor R defining such a rotation is:

$$R = \cos\left(\frac{\theta}{2}\right) - \sin\left(\frac{\theta}{2}\right)B, \tag{12}$$

where B is the unit bivector, i.e., $B^2 = -1$, representing the plane normal to ℓ . The rotated point \mathbf{x}' is calculated by sandwiching \mathbf{x} between R and its reverse \tilde{R} :

$$\mathbf{x}' = R\mathbf{x}\tilde{R} \tag{13}$$

where

$$\tilde{R} = \cos\left(\frac{\theta}{2}\right) + \sin\left(\frac{\theta}{2}\right)B \tag{14}$$

and $R\tilde{R} = 1$. Furthermore, equation (13) can be extended to arbitrary multivectors. In addition, to specify what unit multivectors are, a norm is defined in \mathcal{G}_n .

For an arbitrary multivector A , it is:

$$\|A\| = \sqrt{\langle A\tilde{A} \rangle_0}, \quad (15)$$

where $\langle \cdot \rangle_0$ is the grade-0 projection operator, i.e., it extracts the scalar elements of the argument multivector.

It will be seen in the following subsection that translations can also be described by *rotors* in the *conformal geometric algebra*, a five-dimensional representation of three-dimensional Euclidean space. In addition, general geometric entities (such as points, lines, planes, circles, etc.) and the relations between them are also easily described in conformal geometric algebra.

2.2.2. Conformal geometric algebra

The conformal model extends the real vector space \mathbb{R}^3 by adding two extra basis vectors, e and \bar{e} , with the property:

$$e^2 = 1, \quad \bar{e}^2 = -1. \quad (16)$$

The enlarged vector space is usually denoted by $\mathbb{R}^{4,1}$. In addition, these two extra vectors allow us to define two null vectors, i.e., vectors whose square vanishes:

$$n_0 = \frac{1}{2}(\bar{e} - e), \quad n_\infty = \bar{e} + e, \quad (17)$$

where n_∞ is associated with the point at infinity and n_0 with the origin. However, in order to avoid confusion with the number of DoF of the robot, denoted by n , an alternative yet accepted notation will be used throughout the rest of the paper:

$$e_0 = \frac{1}{2}(\bar{e} + e), \quad e_\infty = \bar{e} - e, \quad (18)$$

where, again, e_∞ is associated with the point at infinity and e_0 with the origin,

Thus, the conformal geometric algebra of \mathbb{R}^3 is denoted by $\mathcal{G}_{4,1}$ and can be seen as a geometric algebra of higher dimension (specifically, the geometric algebra of $\mathbb{R}^{4,1}$). Now, the two null vectors e_∞ and e_0 allow an intuitive description of translations, that are formulated through *translators* as follows:

$$T_v = 1 - \frac{\mathbf{v}e_\infty}{2}, \quad (19)$$

where the translation is performed in the direction of $\mathbf{v} \in \mathbb{R}^3$. Since $(\mathbf{v}e_\infty)^2 = 0$, translators can be seen as rotors in which the bivector squares to zero. Thus, the translation of an element $A \in \mathcal{G}_{4,1}$ is done as with spatial rotations:

$$A' = T_v A \tilde{T}_v, \quad (20)$$

where:

$$\tilde{T}_v = 1 + \frac{\mathbf{v}e_\infty}{2}. \quad (21)$$

One of the most important advantages of conformal geometric algebra is that it provides a homogeneous model for the n -dimensional Euclidean space. In particular, every point $\mathbf{x} \in \mathbb{R}^3$ is associated with a null vector of $\mathcal{G}_{4,1}$ (including the origin and the point at the infinity). This is done via the Hestenes' embedding:

$$X = H(\mathbf{x}) = \frac{1}{2}\mathbf{x}^2\mathbf{e}_\infty + \mathbf{e}_0 + \mathbf{x}, \quad (22)$$

where X is said to be the *null vector representation* of \mathbf{x} . Now, we can easily deduce the following relation [32]:

$$X_1 \cdot X_2 = -\frac{1}{2}d(\mathbf{x}_1, \mathbf{x}_2)^2, \quad (23)$$

where X_1, X_2 are the null vector representations of $\mathbf{x}_1, \mathbf{x}_2 \in \mathbb{R}^3$ and $d(\cdot, \cdot)$ denotes the Euclidean distance. As a consequence, the distance between two null vectors of $\mathcal{G}_{4,1}$ can be defined via the Euclidean distance:

$$d(X_1, X_2) = \sqrt{-2(X_1 \cdot X_2)}. \quad (24)$$

The relation (23) gives us a way to define geometric objects as elements of $\mathcal{G}_{4,1}$. Let O be a geometric object, then k is said to be the *inner representation* of O if for every point $\mathbf{x} \in O$, $H(\mathbf{x}) \cdot k = 0$. Now, using the relation (10), we have that $0 = (X \cdot k)^* = X \wedge k^*$ so k^* is also a representation of O . In this case, we say that k^* is the *outer representation* of O and, in order to avoid confusion, we will denote it by K .

Now, for two different geometric objects O_1 and O_2 with outer (inner) representations K_1 and K_2 (k_1 and k_2), we define its *meet* or *intersection* $k_1 \vee k_2$ as the multivector

$$k_1 \vee k_2 = (k_1 \wedge k_2)^* = k_1 \cdot K_2. \quad (25)$$

Analogously, if the outer representations of O_1 and O_2 have the same grade, the angle defined by them is computed as follows:

$$\angle(O_1, O_2) = \cos^{-1} \left(\frac{K_1 \cdot K_2}{|K_1||K_2|} \right). \quad (26)$$

To describe the geometric objects we are going to use throughout this work, let $\mathbf{p}_1, \mathbf{p}_2, \mathbf{p}_3, \mathbf{p}_4 \in \mathbb{R}^3$ be four different points with null vector representation $P_1, P_2, P_3, P_4 \in \mathcal{G}_{4,1}$. Then:

- $B = P_i \wedge P_j$ (with $1 \leq i \neq j \leq 4$) is a bivector and the outer representation of the pair of points \mathbf{p}_i and \mathbf{p}_j .
- $L = P_i \wedge P_j \wedge \mathbf{e}_\infty$ (with $1 \leq i \neq j \leq 4$) is a trivector and the outer representation of the line with direction \mathbf{p}_i to \mathbf{p}_j . Its inner representation is the bivector $\ell = \mathbf{v}e_{123} - (\mathbf{p}_i \wedge \mathbf{v})e_{123}\mathbf{e}_\infty$, where $\mathbf{v} = \mathbf{p}_j - \mathbf{p}_i$ is its direction vector.

- $C = P_i \wedge P_j \wedge P_k$ (with $1 \leq i \neq j \neq k \leq 4$) is a trivector and the outer representation of a circle passing through the points $\mathbf{p}_i, \mathbf{p}_j$ and \mathbf{p}_k . Its inner representation is the bivector $c = \pi \wedge s$, where π and s are the inner representations of the plane and sphere whose intersection defines the circle.
- $\Pi = P_i \wedge P_j \wedge P_k \wedge e_\infty$ (with $1 \leq i \neq j \neq k \leq 4$) is a 4-vector and the outer representation of a plane passing through the points $\mathbf{p}_i, \mathbf{p}_j$ and \mathbf{p}_k . Its inner representation is the vector $\pi = \mathbf{n} + \delta e_\infty$, where \mathbf{n} denotes the vector normal to the plane and δ , its orthogonal distance to the origin.
- $S = P_1 \wedge P_2 \wedge P_3 \wedge P_4$ is a 4-vector and the outer representation of a sphere passing through the points $\mathbf{p}_1, \mathbf{p}_2, \mathbf{p}_3$ and \mathbf{p}_4 . Its inner representation is the vector $s = Z - \frac{1}{2}r^2 e_\infty$, where Z is the null vector representation of the center of the sphere and r , its radius.

3. A conformal geometric algebra formulation of forward kinematics

The conformal model of the three-dimensional Euclidean space $\mathcal{G}_{4,1}$ provides an elegant and compact way of describing the forward kinematics. Contrary to the classical approach, where we use the homogeneous transformation matrices constructed with the D-H parameters, this approach is entirely based on the use of rotors.

As stated in section 1, each joint frame is described with respect to the preceding one, i.e., the i -th joint frame is constructed from the $(i-1)$ -th joint frame by the successive application of rigid motions (translations and rotations). Since both are described in $\mathcal{G}_{4,1}$ by rotors, for each joint i , the following rotors are defined:

$$\begin{aligned}
T_{d_i} &= 1 - d_i \frac{z_i e_\infty}{2}, \\
R_{\theta_i} &= \cos\left(\frac{\theta_i}{2}\right) - \sin\left(\frac{\theta_i}{2}\right) \mathbf{x}_i \wedge \mathbf{y}_i, \\
T_{a_i} &= 1 - a_i \frac{\mathbf{x}_{i-1} e_\infty}{2}, \\
R_{\alpha_i} &= \cos\left(\frac{\alpha_i}{2}\right) - \sin\left(\frac{\alpha_i}{2}\right) \mathbf{y}_{i-1} \wedge \mathbf{z}_{i-1}.
\end{aligned} \tag{27}$$

where $\{\mathbf{x}_i, \mathbf{y}_i, \mathbf{z}_i\}$ (resp. $\{\mathbf{x}_{i-1}, \mathbf{y}_{i-1}, \mathbf{z}_{i-1}\}$) denotes the three basis elements of the i -th (resp. $(i-1)$ -th) joint frame. Then, two main rotors can be constructed from the previous ones:

$$\begin{aligned}
M_{\theta_i} &= T_{d_i} R_{\theta_i}, \\
M_{\alpha_i} &= T_{a_i} R_{\alpha_i}.
\end{aligned} \tag{28}$$

Notice that rotor M_{θ_i} contains both joint variables, while M_{α_i} is a constant rotor. M_{θ_i} represents a screw motion around the i -th joint axis, \mathbf{z}_i , while M_{α_i} represents a screw motion around the \mathbf{x}_{i-1} axis of the $(i-1)$ -th joint frame.

Now, we can formulate the forward kinematics of a serial robot of n DoF as follows:

$$X' = M_{\theta_1} M_{\alpha_1} \cdots M_{\theta_n} M_{\alpha_n} X \widetilde{M}_{\alpha_n} \widetilde{M}_{\theta_n} \cdots \widetilde{M}_{\alpha_1} \widetilde{M}_{\theta_1}, \quad (29)$$

where X' (X) is the null vector representation of either the end-effector (reference frame) position vector or the vectors defining the end-effector (reference frame) orientation. We can compactly rewrite identity (29) as follows:

$$X' = M_1(q_1) \cdots M_n(q_n) X \widetilde{M}_n(q_n) \cdots \widetilde{M}_1(q_1) = M(\mathbf{q}) X \widetilde{M}(\mathbf{q}), \quad (30)$$

where $M(\mathbf{q}) = M_1(q_1) \cdots M_n(q_n)$ and $M_i(q_i) = M_{\theta_i} M_{\alpha_i}$. Basically, what we are doing is to transform the fixed reference frame (usually placed at the base of the robot) into the end-effector frame according to configuration \mathbf{q} .

4. Pose representation in conformal geometric algebra

If the desired end-effector pose is represented in matrix form as:

$$T = \begin{pmatrix} R & \mathbf{p} \\ 0 & 1 \end{pmatrix}, \quad (31)$$

then it is possible to construct a rotor $M \in \mathcal{G}_{4,1}$ that also represents such a pose. Indeed, given the matrix representation of the reference frame:

$$T_0 = \begin{pmatrix} I_3 & 0 \\ 0 & 1 \end{pmatrix}, \quad (32)$$

we can compute the rotor that transforms T_0 into T . First, the position vector \mathbf{p} defines the rotor:

$$T_{\mathbf{p}} = 1 - \|\mathbf{p}\| \frac{\mathbf{p}e_{\infty}}{2}, \quad (33)$$

that applied to e_0 give us $P = e_0 + \mathbf{p} + \frac{1}{2}\mathbf{p}^2 e_{\infty}$, i.e., the null vector representation of \mathbf{p} . Now, to compute the rotor that relates the orientations determined by the rotation matrices R and I_3 , we notice that both rotation matrices can be seen as two sets of orthogonal vectors in \mathbb{R}^3 , namely $\{e_1, e_2, e_3\}$ and $\{f_1, f_2, f_3\}$. Then, the problem is reduced to find a rotor transforming one set of orthogonal vectors into another. In [31, pag. 103], a simple way of computing such rotor is presented. It involves the use of the *reciprocal frame*. Associated with any arbitrary set of orthogonal vectors $\{e_1, \dots, e_n\}$, there exists another set of orthogonal vectors, denoted by $\{e^1, \dots, e^n\}$ and defined by the property:

$$e^i \cdot e_j = \delta_{ij} \text{ for all } i, j = 1, \dots, n, \quad (34)$$

where δ_{ij} denotes the Kronecker δ . Such a set is said to be the reciprocal frame of $\{e_1, \dots, e_n\}$.

Now, following [31, pag. 103], the following formula is established:

$$R_{I_3, R} = \frac{1 + f_1 e^1 + f_2 e^2 + f_3 e^3}{|1 + f_1 e^1 + f_2 e^2 + f_3 e^3|}, \quad (35)$$

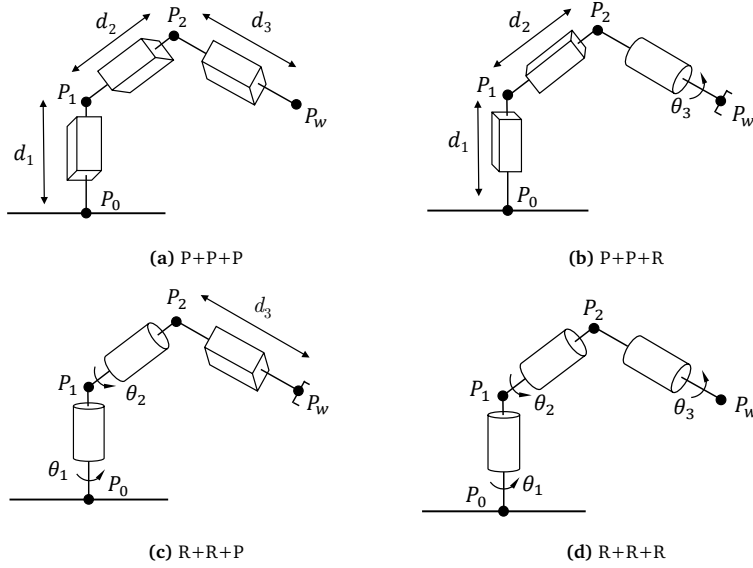


Figure 2: Different combinations of the joints forming the position part of a serial robot with a spherical wrist. Here, R denotes a revolute joint and P denotes a prismatic joint.

where, again, $\{e_1, e_2, e_3\}$ is the orientation of the reference frame, while $\{f_1, f_2, f_3\}$ is the desired orientation of the end-effector. Finally, the rotor M that transforms T_0 into T is the product of rotors (33) and (35):

$$M = T_p R_{I_3, R}. \quad (36)$$

As stated in section 1, for any serial robot with a spherical wrist, the target position \mathbf{p} can be moved to the wrist center point \mathbf{p}_w by a fixed transformation. Then, the new target position is \mathbf{p}_w and thus, it can be assured that the first three joints contribute to the position and orientation, while the last three only contribute to the orientation. This allows us to decouple the inverse kinematics into the position and the orientation subproblems.

5. Solutions for non-redundant robots with spherical wrist

In this section, the position and orientation problems for a 6 DoF serial robot with a spherical wrist are solved. Again, for the position problem different geometric strategies are defined depending on the nature and disposition of the joints along the kinematic chain. For the orientation problem, the rotor $R_{I_3, R}$ is split into three different rotors from which the joint variables can be obtained.

5.1. Position problem

Four different combinations of prismatic and revolute joints that constitute the position part of the robot are analysed (figure 2). For each of them, a geo-

metric strategy is developed. It consists of computing the null vector representation of some auxiliary points placed at each joint to recover the corresponding joint variables as the angle or displacement between two geometric objects defined with such points. For each case, the point at the origin, e_0 , is denoted by P_0 and is placed at the base of the robot. Similarly, the target position \mathbf{p}_w is expressed as a null vector, P_w , obtained through the Hestenes' embedding (22). Finally, depending on the information available, for a given geometric object it could be convenient to use its inner representation k or its outer representation K . Clearly, a geometric object described with one of these two representations can be expressed in the other representation by using the dual operator (as explained in section 2.2.2):

$$K = I_5 k. \quad (37)$$

5.1.1. Three prismatic joints ($P+P+P$)

A scheme of the position part of a serial robot with three prismatic joints is depicted in figure 2a. First of all, the case without offsets between consecutive joints is considered, i.e., the axes of each pair of consecutive joints intersect. Given the first translation axis \mathbf{z}_1 , two of the rotors defined in (27) can be used to obtain the joint axes \mathbf{z}_2 and \mathbf{z}_3 as follows:

$$\begin{aligned} \mathbf{z}_2 &= R_{\theta_2} R_{\alpha_2} \mathbf{z}_1 \tilde{R}_{\alpha_2} \tilde{R}_{\theta_2}, \\ \mathbf{z}_3 &= R_{\theta_3} R_{\alpha_3} \mathbf{z}_2 \tilde{R}_{\alpha_3} \tilde{R}_{\theta_3}. \end{aligned} \quad (38)$$

The joint axis \mathbf{z}_3 together with the target position \mathbf{p}_w defines a line whose inner representation is:

$$\ell_3 = \mathbf{z}_3 e_{123} - (\mathbf{p}_w \wedge \mathbf{z}_3) e_{123} e_\infty. \quad (39)$$

Now, a plane containing the joint axes \mathbf{z}_1 and \mathbf{z}_2 and passing through the point P_0 is also defined so its inner representation is:

$$\pi_1 = \mathbf{z}_1 \times \mathbf{z}_2, \quad (40)$$

where \times denotes the cross product between three-dimensional vectors.

Since the end-effector position is not restricted to a fixed plane, there are not parallel prismatic joint axes. Moreover, $\mathbf{z}_1 \wedge \mathbf{z}_2 \wedge \mathbf{z}_3 \neq 0$ and, thus, the intersection of the line and plane represented by ℓ_3 and π_1 is non-empty (as graphically shown in figure 3a):

$$B = \ell_3 \vee \pi_1, \quad (41)$$

where $B \neq 0$ is a bivector (as deduced from identity (25)). Hence, it represents a pair of points in conformal geometric algebra. However, since the intersection between a line and a plane is a single point, the bivector B is of the form:

$$B = P_2 \wedge e_\infty \quad (42)$$

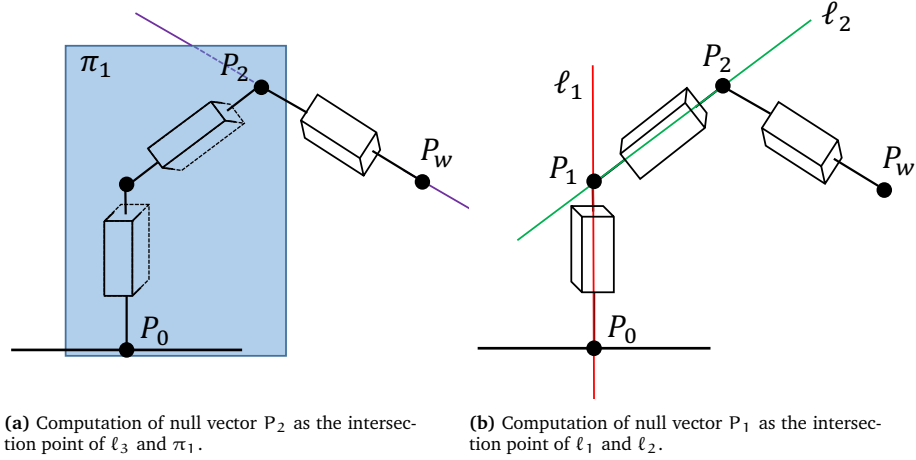


Figure 3: Geometric computation of the null vectors P_2 and P_1 .

for a null point P_2 , that can be extracted from B as explained in [34, pags. 24-26]. With this null point, the following lines are defined through their inner representations:

$$\begin{aligned} \ell_1 &= z_1 e_{123} - (e_0 \wedge z_1) e_{123} e_\infty, \\ \ell_2 &= z_2 e_{123} - (\mathbf{p}_2 \wedge z_2) e_{123} e_\infty, \end{aligned} \quad (43)$$

where \mathbf{p}_2 is the vector whose null vector representation is P_2 and that is recovered with the projection $P : \mathbb{R}^{4,1} \rightarrow \mathbb{R}^3$, that is, the inverse of the Hestenes' embedding (22). In addition, if L_1, L_2 and Π_1 are the outer representations of the two lines and plane defined before, $L_1 \wedge \Pi_1 = 0$ and $L_2 \wedge \Pi_1 = 0$ and, since the joint axes z_1 and z_2 are not parallel, they have non-empty intersection. This can be seen depicted in figure 3b. However, this intersection is a special case. Indeed

$$\ell_1 \vee \ell_2 = (\ell_1 \wedge \ell_2)^* \quad (44)$$

is a grade one element, i.e., a vector. Non-null vectors do not represent any geometric object in conformal geometric algebra. Therefore, we need an alternative method for obtaining the intersection point. In this paper, we follow the same technique as in [34, pag. 31] to compute $P_1 = \ell_1 \vee \ell_2$.

Finally, with the null vectors P_0, P_1, P_2 and P_w , the joint variables are recovered using the distance (24):

$$d_1 = d(P_0, P_1), d_2 = d(P_1, P_2) \text{ and } d_3 = d(P_2, P_w). \quad (45)$$

Now, the case where there is an offset between two consecutive joints is studied. Offsets are always modeled by the four D-H parameters a, α, θ and d . If joint i is revolute (prismatic), its joint variable can have an offset as well (aligned with the joint axis by definition). In that case, we write $\theta_i = \hat{\theta}_i + \bar{\theta}_i$ ($d_i = \hat{d}_i + \bar{d}_i$), where $\hat{\theta}_i$ (\hat{d}_i) denotes the real joint variable and $\bar{\theta}_i$ (\bar{d}_i), the length of the offset.

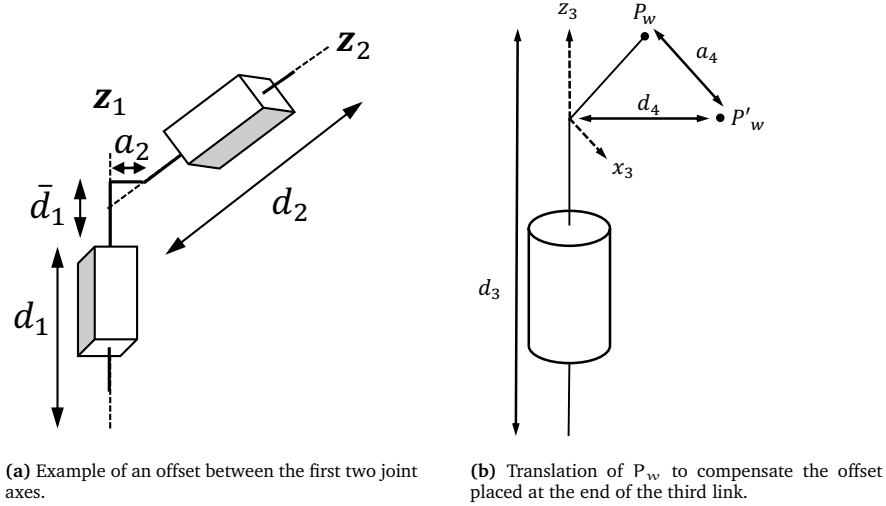


Figure 4: Offsets in the position part of serial robots with spherical wrist.

Let us suppose, without loss of generality, that there exists an offset of fixed length between the first two joints (the other cases are analogous). Clearly, such offset is either aligned with the common perpendicular between the first and second joint axes and has length a_2 or can be decomposed into two components (as depicted in figure 4a): one aligned with such a common perpendicular (with length a_2) and the other one aligned with the first joint axis (with length \bar{d}_1). Now, since the plane represented by π_1 is defined with the joint axes z_1 and z_2 and, in this case, offsets do not change the direction of the joint axes, we can translate it in the direction of the common perpendicular by an amount equal to a_2 :

$$\pi'_1 = T_{a_2} \pi_1 \tilde{T}_{a_2}, \quad (46)$$

where T_{a_2} is defined as in (27). Now, $P_2 \in \pi'_1$ and, therefore, P_2 can be obtained from equation (41) as in the case without offsets. With P_2 , the inner representation ℓ_2 of a line is determined as in (43). Then, this line is transformed as follows:

$$\ell'_2 = T_{-\bar{d}_1} T_{-a_2} \ell_2 \tilde{T}_{-a_2} \tilde{T}_{-\bar{d}_1}, \quad (47)$$

where, again, T_{-a_2} and $T_{-\bar{d}_1}$ are defined as in (27). Now, since the lines represented by ℓ_1 and ℓ'_2 belong to the same plane, they have non-empty intersection and $P_1 = \ell_1 \vee \ell'_2$. This completes the solution for this case.

5.1.2. Two prismatic joints and one revolute (P+P+R)

The position part of a serial robot with two prismatic joints and one revolute is depicted in figure 2b. There are different combinations of two prismatic joints with one revolute but most of them are treated in a similar way. Only the most relevant cases are fully developed here. Again, the case without offsets is considered first.

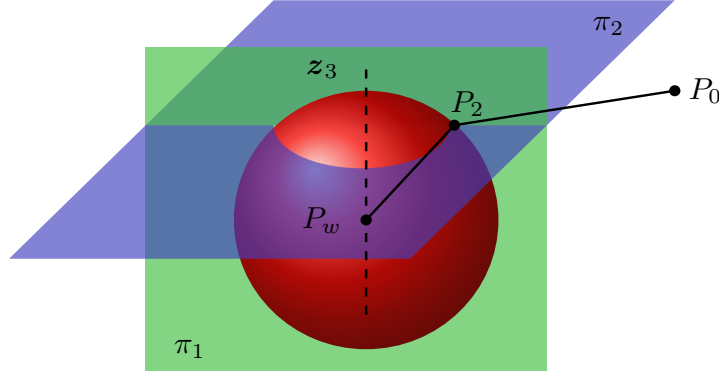


Figure 5: P_2 as the intersection of two planes and one sphere.

Let us suppose that the first two joints are prismatic and the third one, revolute. As in the preceding case, given z_1 , the joint axes z_2 and z_3 can be calculated as in (38). Now, the inner representation of the plane that contains P_0 and the joint axes z_1 and z_2 is defined as in (40) and denoted by π_1 . Since the robot has 6 DoF, its end-effector position is not restricted to a fixed plane and, thus, there exists an offset at the end of the third link, i.e., between the third link and the set of joints that forms the spherical wrist. In addition, z_3 cannot be orthogonal to the plane represented by π_1 (if it was, \mathbf{p}_w would always belong to a fixed plane parallel to the plane represented by π_1).

Since the last three joints of the robot do not contribute to the position of the end-effector, they are not considered in the position problem. Therefore, this offset can be seen as a displacement defined in the x - z plane of the third joint frame, i.e., a displacement of length a_4 in the x_3 direction. Then, it is possible to translate P_w to compensate the offset (as depicted in figure 4b):

$$P'_w = T_{-a_4} P_w \tilde{T}_{-a_4}, \quad (48)$$

where T_{-a_4} is defined as in (27). Now, the null point P_2 belongs to the intersection of two planes with one sphere. One of these planes is represented by π_1 , while the other is defined as follows:

$$\pi_2 = z_3 + d(P_0, P'_w)e_\infty. \quad (49)$$

Additionally, the inner representation of the sphere is defined as:

$$s_1 = P'_w - \frac{1}{2}(d_3^2 + d_4^2)e_\infty, \quad (50)$$

where d_3 denotes the length of the third link and d_4 , the distance between the origin of the third frame and \mathbf{p}_w measured in the direction of the z_4 axis.

Since the plane represented by π_2 does not contain P_2 , we translate it in the z_3 direction:

$$\pi'_2 = T_{d_3} \pi_2 \tilde{T}_{d_3}, \quad (51)$$

where

$$T_{d_3} = 1 - d_3 \frac{z_3 e_\infty}{2}. \quad (52)$$

The intersection of these geometric objects is graphically depicted in figure 5 and is computed as:

$$B = \pi_1 \vee \pi'_2 \vee s_1, \quad (53)$$

where B is a bivector. Again, this bivector represents a pair of points in the conformal geometric algebra $\mathcal{G}_{4,1}$ so:

$$B = Q_1 \wedge Q_2, \quad (54)$$

for some null points Q_1 and Q_2 . Clearly, if Q_1 and Q_2 belong to the workspace \mathcal{W} of the robot, then there are two possible null points P_2 , namely $P_{21} = Q_1$ and $P_{22} = Q_2$. Therefore, we have two possible valid positions for the null point lying between the second and the third joint. As we will see, this means that, in this case, there are more than one set of solutions. Each one of these two null points defines a line whose inner representation, ℓ_{21} (ℓ_{22}) if P_{21} (P_{22}) is used, is computed as in (43). Similarly, the inner representation ℓ_1 of another line is calculated as in (43). Now, two distinct null points P_1 can be obtained. Indeed, for $i = 1, 2$, $P_{1i} = \ell_{2i} \vee \ell_1$.

Finally, each pair of null points $\{P_{11}, P_{21}\}$ and $\{P_{12}, P_{22}\}$ allows us to compute the outer representation of an extra plane that is used to calculate the joint variable θ_3 :

$$\begin{aligned} \Pi_{31} &= P_{11} \wedge P_{21} \wedge P'_w \wedge e_\infty, \\ \Pi_{32} &= P_{12} \wedge P_{22} \wedge P'_w \wedge e_\infty. \end{aligned} \quad (55)$$

Then, using the identities (23) and (26), the joint variables d_1 , d_2 and θ_3 can be derived easily. Clearly, we are going to have two different sets of joint variables and, therefore, two different solutions:

$$\begin{aligned} d_{11} &= d(P_0, P_{11}), d_{21} = d(P_{11}, P_{21}) \text{ and } \theta_{31} = \angle(\Pi_1, \Pi_{31}), \\ d_{12} &= d(P_0, P_{12}), d_{22} = d(P_{11}, P_{22}) \text{ and } \theta_{32} = \angle(\Pi_1, \Pi_{32}). \end{aligned} \quad (56)$$

As stated in section 1, serial robots with 6 DoF and spherical wrist have up to eight distinct solutions for a given end-effector pose. Since the orientation problem always has two different solutions for each solution of the position problem, there is a maximum of four distinct solutions for the position problem. This maximum is reached only in two cases: (1) when the three joints that constitute the position part of the robot are revolute and (2) when the two of the three joints that constitute the position part of the robot are revolute and the other one is prismatic. Therefore, this case shows how the geometric strategy introduced in this paper gives all the solutions for the inverse kinematics and,

thus, it can be considered a closed-form method. However, from now on, in order to simplify the notation for the remaining cases, we are going to consider just one of the two points that can be extracted from a given bivector and, hence, only one of the maximum of four different sets of solutions will be fully developed.

Offsets between consecutive joints are treated analogously as in the previous case. The main difference relies on the geometric object considered:

- If the offset is located between the first and the second joint, then P_2 can be derived as in the preceding section, while P_1 is computed as the intersection $\ell_1 \vee \ell'_2$, where ℓ'_2 is defined as in (47).
- If the offset is located between the second and the third joint, then $d_3 = \hat{d}_3 + \bar{d}_3$, where \bar{d}_3 is a component of the offset aligned with the z_3 axis. Now, P_2 is extracted from:

$$B = \pi_1 \vee \pi'_2 \vee s'_1, \quad (57)$$

where $s'_1 = T_{-\bar{d}_3} T_{-\alpha_3} s_1 \tilde{T}_{-\alpha_3} \tilde{T}_{-\bar{d}_3}$ is the inner representation of the sphere represented by s_1 after compensating the offset and $T_{-\alpha_3}, T_{-\bar{d}_3}$ are defined as in (27). Since the remaining geometric reasoning does not change, P_1 is obtained as in the case without offsets. This situation highlights another advantage of conformal geometric algebra: rotors can be applied to any geometric object which simplifies the formulation and the solution of the problem.

Another relevant case is when the first joint is revolutive, while the second and third ones are prismatic. This case is solved in a similar way, but it is interesting to point out some details. First, the null point P_1 is obtained as the translation of P_0 along z_1 an amount equal to the length of the first link, i.e., d_1 . Indeed:

$$P_1 = T_{d_1} P_0 \tilde{T}_{d_1}, \quad (58)$$

with T_{d_1} defined as in (27). Since the second joint is prismatic, θ_2 is one of the known D-H parameters and, hence, the joint axes z_2 and z_3 can be computed as in (38). Now, P_2 is derived as $P_2 = \ell_2 \vee \ell_3$, where ℓ_2 and ℓ_3 are defined as in (39) and (43). The joint variables d_2 and d_3 are determined as in (45). Now, we define the following two planes such as their outer representations are:

$$\begin{aligned} \Pi_1 &= P_0 \wedge P_1 \wedge P'_w \wedge e_\infty, \\ \Pi'_1 &= P_0 \wedge P_1 \wedge P'_w \wedge e_\infty, \end{aligned} \quad (59)$$

where P'_w is the null vector representation of the three-dimensional point \mathbf{p}'_w computed with the obtained values for the joint variables d_2 and d_3 and with $\theta_1 = 0$. Clearly, the first joint variable is obtained as $\theta_1 = \angle(\Pi_1, \Pi'_1)$.

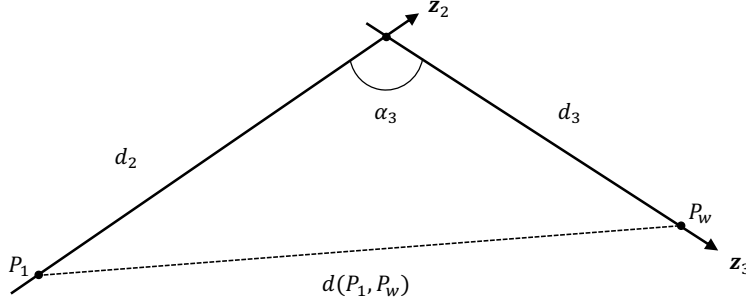


Figure 6: Triangle defined by z_2 and z_3 .

5.1.3. Two revolute joints and one prismatic (R+R+P)

A scheme of the position part of a serial robot with two revolute joints and one prismatic joint is depicted in figure 2c. As in the preceding case, there are different subcases that can be treated similarly. Because of that, only the most relevant cases are fully developed here.

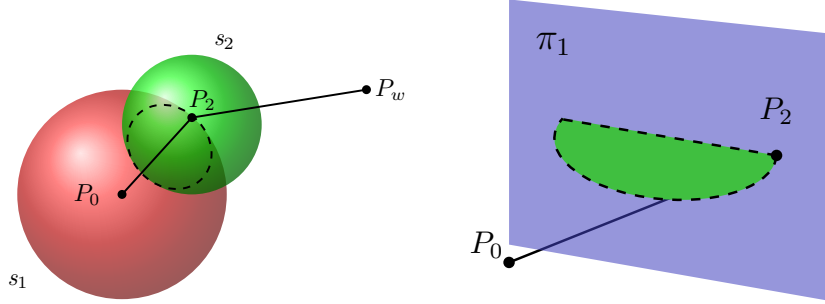
First, let us consider the case where the first two joints are revolute and the third one, prismatic. In addition, for this first case, we suppose that there are no offsets between consecutive joints. The null point P_1 is computed as in (58). Now, the remaining part of the position part of the robot is restricted to the plane determined by the joint axes z_2 and z_3 . Furthermore, given the length of the second link, d_2 , and the angle between the joint axes z_2 and z_3 , α_3 , a triangle as the one depicted in figure 6 is defined. Using the law of cosines, d_3 can be easily obtained from the quadratic equation:

$$d(P_1, P_w)^2 = d_2^2 + d_3^2 - 2d_2d_3 \cos(\alpha_3). \quad (60)$$

Now, since $d(P_1, P_w) > d_2 \sin(\alpha_3)$, equation (60) has always two distinct real solutions. Therefore, we have three different cases: (1) there are two distinct positive solutions; (2) there are two distinct negative solutions and (3) there is one positive and one negative solutions. It is clear that, since the displacements measured by the D-H parameter d are always positive, the case with two distinct negative solutions is undesirable. This case only holds when

$$d_2 > d(P_1, P_w) \text{ and } d_2 \cos(\alpha_3) < 0. \quad (61)$$

But, however, since $d_2 \geq 0$, if $d_2 \cos(\alpha_3) < 0$, then $\cos(\alpha_3) < 0$ and, thus, $\alpha_3 \in [\pi/2, 3\pi/2]$. Nevertheless, for those values of α_3 , $d_2 < d(P_1, P_w)$ by definition of the D-H parameters. This is clearly the opposite of the first inequality of (61), which means that only the cases (1) and (3) are possible. In addition, if there is a fixed offset aligned with the z_3 axis, then d_3 can be decomposed as $d_3 = \hat{d}_3 + \bar{d}_3$, where, as usual, \bar{d}_3 denotes the length of this offset. It is straightforward to see that, also in this case, the joint variable \hat{d}_3 can be obtained from (60).



(a) P_2 lying in the circle intersection of the spheres represented by s_1 and s_2 .

(b) P_2 as the intersection of a circle and the plane represented by π_1 .

Figure 7: Computation of P_2 .

Finally, in order to obtain P_2 , we define two distinct spheres and one plane through their inner and outer representations:

$$\begin{aligned}
 s_1 &= P_1 - \frac{1}{2}d_2^2 e_\infty, \\
 s_2 &= P_w - \frac{1}{2}d_3^2 e_\infty, \\
 \Pi_1 &= P_0 \wedge P_1 \wedge P_w \wedge e_\infty.
 \end{aligned} \tag{62}$$

Then, the intersection of these geometric objects is computed (and shown graphically in figures 7a and 7b):

$$B = s_1 \vee s_2 \vee \pi_1, \tag{63}$$

where two different null points P_2 can be extracted from B . Since we have already computed d_3 , we use the null points P_0, P_1 and P_2 to derive the remaining joint variables, namely θ_1 and θ_2 . The following auxiliary geometric objects are defined for that purpose:

- If the revolute joints have parallel joint axes:

$$L_1 = P_1 \wedge P_2 \wedge e_\infty \text{ and } L_2 = P_2 \wedge P_w \wedge e_\infty. \tag{64}$$

- If the revolute joints have not parallel joint axes:

$$\Pi_2 = P_0 \wedge P_1 \wedge P_2 \wedge e_\infty \text{ and } \Pi_3 = P_1 \wedge P_2 \wedge P_w \wedge e_\infty. \tag{65}$$

Now, for the parallel case, the joint variable θ_2 is computed as follows:

$$\theta_2 = \angle(L_1, L_2). \tag{66}$$

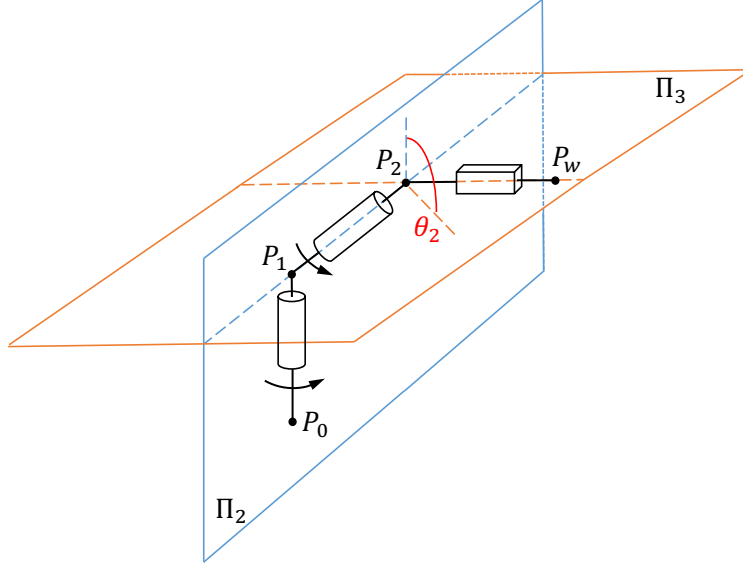


Figure 8: Computation of θ_2 as the angle between Π_2 and Π_3 for the case of non-parallel revolute joint axes.

Since the joint variables θ_2 and d_3 are already known, the position of the end-effector with $\theta_1 = 0$ can be computed. If we denoted such a three-dimensional point \mathbf{p}'_w , we can define an extra plane whose outer representations is:

$$\Pi'_1 = P_0 \wedge P_1 \wedge P'_w \wedge e_\infty, \quad (67)$$

where P'_w is the null vector representation of \mathbf{p}'_w . Now, $\theta_1 = \angle(\Pi_1, \Pi'_1)$. For the other case (shown graphically in figure 8), we have that:

$$\theta_2 = \angle(\Pi_2, \Pi_3), \quad (68)$$

where, again, θ_1 is computed as $\theta_1 = \angle(\Pi_1, \Pi'_1)$, where Π'_1 is defined with the already obtained values of θ_2 and d_3 and with $\theta_1 = 0$.

Offsets are treated analogously to the preceding cases. Two different situations arise:

- If the offset is placed between the second and the third joints, then we translate the null point P_w as follows:

$$P'_w = T_{-\tilde{d}_3} T_{-\alpha_3} P_w \tilde{T}_{-\alpha_3} \tilde{T}_{-\tilde{d}_3}, \quad (69)$$

where $T_{-\tilde{d}_3}$ and $T_{-\alpha_3}$ are defined as in (27). Now, the rest of the reasoning is as in the case without offsets. The null point P_1 is calculated as in (58) and, hence, a triangle such as the one depicted in figure 6 can be defined using, instead of P_w , P'_w .

- If the offset is placed between the first and the second joints, we can simply translate the null point P_0 in the direction \mathbf{x}_1 and amount equal to a_2 , i.e., to compute $P'_0 = T_{a_2} P_0 \tilde{T}_{a_2}$, where T_{a_2} is defined as in (27). The remaining steps are as in the case without offsets, using P'_0 instead of P_0 .

Finally, let us consider another subcase: the first joint is revolute, the second joint is prismatic and the third joint is again revolute. The null points P_0 and P_1 are obtained as in the preceding case. To calculate the null point P_2 , the geometric reasoning used for the case where there are two prismatic joints followed by one revolute is applied. Therefore, the planes and the sphere represented by π_1, π_2, π_3 and s_1 are defined as in (40),(49),(50) and (55). Finally, the joint variables are obtained as in the above-mentioned case.

5.1.4. Three revolute joints (R+R+R)

A scheme of the position part of a serial robot with three revolute joints is depicted in figure 2d. First, the case without offsets is developed.

As in the preceding case, the null point P_1 is computed as $P_1 = T_{a_1} P_0 \tilde{T}_{a_1}$, where T_{a_1} is defined as in (27). Once P_1 has been obtained, the null point P_2 is computed by intersecting two spheres and one plane whose outer and inner representations are:

$$\begin{aligned} \Pi_1 &= P_0 \wedge P_1 \wedge P_w \wedge e_\infty, \\ s_1 &= P_1 - \frac{1}{2} a_2^2 e_\infty, \\ s_2 &= P_w - \frac{1}{2} (a_3 + d_3)^2 e_\infty. \end{aligned} \tag{70}$$

The intersection of these three geometric objects is, again, a bivector:

$$B = s_1 \vee s_2 \vee \pi_1, \tag{71}$$

where, as in the preceding cases, two different points P_2 can be extracted from B , each one leading to a different solution.

Now, two distinct cases are considered to obtain the joint variables: two joint axes are parallel or no joint axes are parallel. The case where the three joint axes are parallel is not considered because it will mean that the position problem is a two-dimensional problem instead of a three-dimensional one, i.e., that the robot has less than 6 DoF. Hence:

- If there are two joints whose joint axes are parallel, then let us suppose that the two parallel joint axes are the last two (the other cases are analogous). Then, the outer representation of the geometric objects required for computing the joint variables are defined as:

$$\begin{aligned} L_1 &= P_0 \wedge P_1 \wedge e_\infty, \\ L_2 &= P_1 \wedge P_2 \wedge e_\infty, \\ L_3 &= P_2 \wedge P_w \wedge e_\infty, \end{aligned} \tag{72}$$

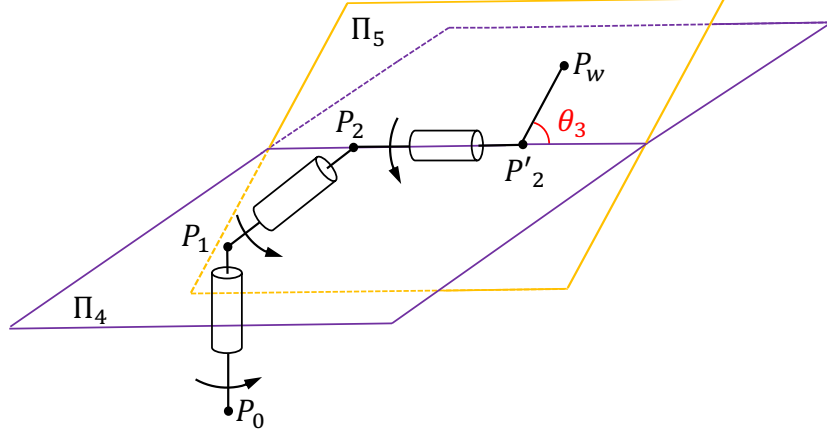


Figure 9: Computation of θ_3 as the angle between Π_4 and Π_5 for the case of non-parallel revolute joint axes.

and the joint variables are:

$$\theta_1 = \angle(\mathbf{x}_1, \Pi_1), \theta_2 = \angle(L_1, L_2) \text{ and } \theta_3 = \angle(L_2, L_3), \quad (73)$$

where $\angle(\mathbf{x}_1, \Pi_1)$ cannot be computed using equation (26) since it is only defined for blades of the same grade. However, the following relation holds:

$$\angle(\mathbf{x}_1, \Pi_1) = \frac{\pi}{2} - \angle(\mathbf{n}, \mathbf{x}_1), \quad (74)$$

where \mathbf{n} is the vector normal to Π_1 (and can be easily retrieved from its inner representation π_1), so the computation of $\angle(\mathbf{x}_1, \Pi_1)$ reduces to the computation of $\angle(\mathbf{x}_1, \mathbf{n})$. Interestingly, this coincides with the approach followed in [21, 24].

- If there are no revolute joints with parallel joint axes, we have that:

$$\begin{aligned} \Pi_2 &= P_0 \wedge P_1 \wedge P_2 \wedge e_\infty, \\ \Pi_3 &= P_1 \wedge P_2 \wedge P_w \wedge e_\infty, \end{aligned} \quad (75)$$

and, therefore:

$$\theta_2 = \angle(\Pi_2, \Pi_3). \quad (76)$$

Then, once θ_2 is computed, the joint axis of the second joint, z_2 , can be computed from the three-dimensional points \mathbf{p}_1 and \mathbf{p}_2 (which are the Euclidean points whose null vector representation are P_1 and P_2 respectively). Now, z_3 is calculated as in (38) and we translate the null vector P_2 along z_3 an amount equal to α_3 :

$$P'_2 = T_{\alpha_3} P_2 \tilde{T}_{\alpha_3}. \quad (77)$$

This extra null vector allows us to define two additional planes:

$$\begin{aligned}\Pi_4 &= P_1 \wedge P_2 \wedge P'_2 \wedge e_\infty, \\ \Pi_5 &= P_2 \wedge P'_2 \wedge P_w \wedge e_\infty,\end{aligned}\tag{78}$$

which, in turn, allow us to compute θ_3 as follows:

$$\theta_3 = \angle(\Pi_4, \Pi_5).\tag{79}$$

This is graphically depicted in figure 9. Finally, θ_1 is computed as in the previous cases.

Finally, the offsets are treated by transforming the proper geometric object. For instance, if the offset is placed between the first and the second joint, then P_0 is transformed into $P'_0 = T_{a_2} P_0 \tilde{T}_{a_2}$, where T_{a_2} is defined as in (27). Then, the remaining steps are as in the case without offsets using P'_0 instead of P_0 . If, conversely, the offset is placed between the second and the third joint, then the sphere represented by s_2 is transformed into $s'_2 = T_{-a_3} s_2 \tilde{T}_{-a_3}$, where, again, T_{-a_3} is computed as in (27). Therefore, the null point P_2 is extracted from the intersection bivector $\pi_1 \vee s_1 \vee s'_2$ and the remaining steps are the same as the ones in the case without offsets.

5.2. Solution of the orientation problem

Once the position problem is solved, the value of the joint variables q_1, q_2, q_3 is known and it only remains to find q_4, q_5 and q_6 . With q_1, q_2, q_3 , we compute the rotor defining the orientation of the frame attached to \mathbf{p}_w under the effect of these joints and we denote it by R_{123} . Now, recall that $R_{I_3, R}$ denotes the rotor representing the target orientation of the end-effector. Then, the rotor that defines the rotation between R_{123} and $R_{I_3, R}$ can be obtained from the relation (figure 10):

$$R_{I_3, R} = R_{123} R_{456},\tag{80}$$

where the rotor R_{456} only depends on the joint variables q_4, q_5 and q_6 . Since these joints are revolute, q_4, q_5 and q_6 correspond to θ_4, θ_5 and θ_6 , respectively.

Now, we split R_{456} into three different rotors as follows:

$$R_{456} = R_4 R_5 R_6,\tag{81}$$

where:

$$R_i = \cos\left(\frac{\theta_i}{2}\right) - \sin\left(\frac{\theta_i}{2}\right) B_i,\tag{82}$$

where θ_i is the angle of rotation B_i is the bivector defining the rotation plane. Clearly, the angle extracted from each one of these rotors will correspond to one of the sought joint variables. We expand (81) and obtain:

$$\begin{aligned}R_{456} = R_4 R_5 R_6 &= c_4 c_5 c_6 - c_4 c_6 s_5 B_5 - c_5 c_6 s_4 B_4 - c_4 c_5 s_6 B_6 + \\ &+ c_6 s_4 s_5 B_4 B_5 + c_4 s_5 s_6 B_5 B_6 + c_5 s_4 s_6 B_4 B_6 - s_4 s_5 s_6 B_4 B_5 B_6,\end{aligned}\tag{83}$$

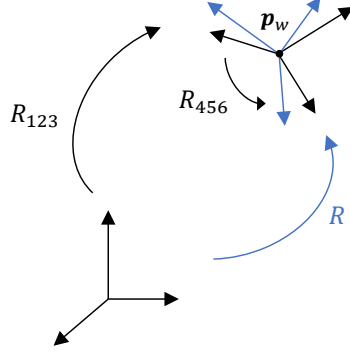


Figure 10: Relation between the orientations

where $c_i = \cos(\theta_i/2)$ and $s_i = \sin(\theta_i/2)$. In addition, R_{456} can also be written:

$$R_{456} = \cos\left(\frac{\theta}{2}\right) - \sin\left(\frac{\theta}{2}\right)B_{456} \quad (84)$$

for a known angle θ and bivector B_{456} . But, since $R_{I_3, R}$ and R_{123} are rotors in \mathcal{G}_3 (by definition), then R_{456} is also a rotor in \mathcal{G}_3 and, thus, we can write B_{456} as a linear combination with respect to the basis bivectors of \mathcal{G}_3 :

$$B_{456} = \beta_1 e_{23} + \beta_2 e_{13} + \beta_3 e_{12} \quad (85)$$

for some $\beta_1, \beta_2, \beta_3 \in \mathbb{R}$. Then, we can rewrite R_{456} as:

$$R_{456} = \cos\left(\frac{\theta}{2}\right) - \sin\left(\frac{\theta}{2}\right)\beta_1 e_{23} - \sin\left(\frac{\theta}{2}\right)\beta_2 e_{13} - \sin\left(\frac{\theta}{2}\right)\beta_3 e_{12}. \quad (86)$$

Now, as happens with Euler angles, different conventions can be adopted. Depending on the convention used, a particular set of equations is obtained. For instance, by setting

$$B_4 = e_{12}, B_5 = e_{13} \text{ and } B_6 = e_{23}, \quad (87)$$

that corresponds to the Euler angles convention ZYZ , the following relations hold:

$$B_4 B_5 = -e_{23}, B_5 B_6 = e_{23}, B_4 B_6 = -1 \text{ and } B_4 B_5 B_6 = e_{13}. \quad (88)$$

Hence, by regrouping the terms of (83) and equating them to (86), the following set of equations is obtained:

$$\left. \begin{aligned} \alpha &= c_4 c_5 c_6 - c_5 s_4 s_6 \\ \beta'_1 &= c_4 s_5 s_6 - c_6 s_4 s_5 \\ \beta'_2 &= -c_4 c_6 s_5 - s_4 s_5 s_6 \\ \beta'_3 &= -c_5 c_6 s_4 - c_4 c_5 s_6 \end{aligned} \right\} \quad (89)$$

where, again, $c_i = \cos(\theta_i/2)$ and $s_i = \sin(\theta_i/2)$, while $\alpha = \cos(\theta/2)$ and $\beta'_i = -\sin(\theta/2)\beta_i$. Now, by squaring and adding the first and last identities, we obtain:

$$\alpha^2 + (\beta'_3)^2 = \cos^2\left(\frac{\theta_5}{2}\right), \quad (90)$$

and, thus,

$$\theta_5 = \frac{\cos^{-1}\left(\pm\sqrt{\alpha^2 + (\beta'_3)^2}\right)}{2}. \quad (91)$$

Finally, if $\cos(\theta_5/2) \neq 0$ and $\sin(\theta_5/2) \neq 0$, then:

$$\alpha' = \frac{\alpha}{\cos(\theta_5/2)} \quad \text{and} \quad \beta''_2 = \frac{-\beta'_2}{\sin(\theta_5/2)} \quad (92)$$

and, therefore:

$$\theta_6 = \sin^{-1}(\alpha') + \sin^{-1}(\beta''_2) \quad \text{and} \quad \theta_4 = \sin^{-1}(\alpha') - \sin^{-1}(\beta''_2), \quad (93)$$

which completes the resolution of the orientation problem. In case $\theta_5 = 0$ or π , we are in the so-called *representation singularity* of the Euler angles convention ZYZ [2] and, hence, we can only obtain the value of the sum $\theta_4 + \theta_6$. Indeed, from (83) we can easily deduce that $\theta_4 + \theta_6 = 2 \cos^{-1}(\alpha)$ if $\theta_5 = 0$ and $\theta_4 + \theta_6 = 2 \cos^{-1}(-\alpha)$ if $\theta_5 = \pi$.

Although the obtained solutions are equivalent to Euler angles, the advantages of the proposed method are evident. Rotor manipulation is more geometrically intuitive than manipulating Euler angles. In fact, here, rotor manipulation reduces to bivector manipulation, which can be seen as a "linearization" of the problem. In addition, it avoids the use of rotation matrices. Although rotation matrices have good properties that facilitate their computations, they are still more challenging to manipulate than rotors. In addition, their geometric interpretation is not intuitive, while, as stated before, this is the case for rotors.

6. Solutions for redundant robots with spherical wrist

As stated in section 1, there is an infinite number of solutions for the inverse kinematics of redundant serial robots. In [35], redundant robots are reduced to non-redundant ones by the parametrization of the so-called *redundant joints*. Once the analytical solutions for the inverse kinematics have been obtained, particular instances for the parametrized joints are given. Hence, for each instance, a set of a maximum of sixteen solutions is obtained (recall that, for non-redundant robots, this is the upper bound for the number of distinct solutions associated with a given end-effector pose). This can be regarded as the addition of extra conditions in an undetermined problem. Therefore, these particular solutions form a subset of the set of all possible solutions for a given target pose of the end-effector.

Following this idea, the geometric strategies introduced and developed in section 5.1 are extended to serial robots with 7 DoF and spherical wrist. Here, the extra information is given in the form of extra null points P_i that allow the definition of the geometric entities involved in the resolution. As it will be seen in the following cases, the addition of these extra points entails the evaluation of one of the joint variables. In addition, if the identification of the redundant joints developed in [35] is applied to these manipulators, it is possible to know exactly which null points P_i are needed in order to completely solve the position problem.

For each one of the cases studied in the preceding section, an extra degree of freedom – that corresponds either to a prismatic or revolute joint – is added. Several distinct combinations arise, but as in section 5.1, only the most relevant are fully developed in order not to repeat the already used geometric reasonings. In particular, the cases to be considered are: $P+P+P+P$, $P+P+R+P$, $R+R+P+R$ and $R+R+R+R$ where, again, P denotes a prismatic joint and R denotes a revolute joint.

6.1. $P+P+P+P$

The objective is to find P_1, P_2 and P_3 to obtain the joint variables d_1, d_2, d_3 and d_4 . Since all the joints are prismatic, the joint axes z_2, z_3 and z_4 can be calculated as in (38). Now, the inner representation of two distinct planes:

$$\begin{aligned}\pi_1 &= \mathbf{z}_1 \times \mathbf{z}_2, \\ \pi_2 &= \mathbf{z}_3 \times \mathbf{z}_4 + d(P_0, P_w)e_\infty\end{aligned}\quad (94)$$

and two distinct lines is defined:

$$\begin{aligned}\ell_1 &= \mathbf{z}_1 e_{123} - (e_0 \wedge \mathbf{z}_1)e_{123}e_\infty, \\ \ell_2 &= \mathbf{z}_4 e_{123} - (\mathbf{p}_w \wedge \mathbf{z}_4)e_{123}e_\infty.\end{aligned}\quad (95)$$

The intersection of the planes represented by π_1 and π_2 is a line containing the null point P_2 . Indeed, its outer representation is $L_2 = \pi_1 \vee \pi_2$. Now, to determine uniquely P_2 , another plane is needed. Such a plane contains the joint axes z_2 and z_3 . However, it also requires an extra point for setting its distance to P_0 . Let us define P_1 as the null point that verifies:

$$P_1 \wedge L_1 = 0 \quad \text{and} \quad d(P_0, P_1) = d_1. \quad (96)$$

Notice that the definition of P_1 is equivalent to setting d_1 at a particular value. Now, the inner representation of the new plane can be defined as:

$$\pi_3 = \mathbf{z}_2 \times \mathbf{z}_3 + d_1 e_\infty \quad (97)$$

and, therefore, P_2 can be extracted from the intersection bivector $\pi_3 \vee \ell_2$.

Once P_0, P_1 and P_2 have been obtained, P_3 is found as the intersection of the lines represented by ℓ_3 and ℓ_4 , where:

$$\ell_3 = \mathbf{z}_3 e_{123} - (\mathbf{p}_2 \wedge \mathbf{z}_3)e_{123}e_\infty. \quad (98)$$

Again, \mathbf{p}_2 represents the three dimensional vector whose null vector is P_2 and that is recovered using the projection $P : \mathbb{R}^{4,1} \rightarrow \mathbb{R}^3$. Finally, the remaining joint variables d_2, d_3 and d_4 are calculated as in (45).

6.2. $P+P+R+P$

Again, the joint axes \mathbf{z}_2 and \mathbf{z}_3 are calculated as in (38). However, since the third joint is revolute, R_{θ_3} is not a constant rotor and, thus, the joint axis \mathbf{z}_4 cannot be computed. The inner representations of the line ℓ_1 and the plane π_1 are defined as in (94) and (95). Now, an extra point is needed to completely describe the position of \mathbf{z}_4 . Let us denote by P_3 the null point verifying:

$$\angle(\Pi_1, L_3) = \theta_3, \quad (99)$$

where $\ell_3 = \mathbf{z}_3 e_{123} - (\mathbf{p}_3 \wedge \mathbf{z}_3) e_{123} e_\infty$. Since they are represented by blades of different grade, the angle between Π_1 and L_3 cannot be computed using equation (26). However, we can define a line whose outer representation L satisfies:

$$\angle(\Pi_1, L_3) = \frac{\pi}{2} - \angle(L, L_3). \quad (100)$$

Such a line is constructed as follows. The inner representation of Π_1 is $\pi_1 = \mathbf{n} + \delta e_\infty$, where \mathbf{n} denotes the vector normal to the plane. Since Π_1 passes through the origin, its inner representation reduces to $\pi_1 = \mathbf{n}$. Therefore, we can define a line passing also through the origin whose inner representation is $\ell = \mathbf{n} e_{123}$. Finally, its outer representation, $L = I_5 \ell$, gives us the desired line. Furthermore, this definition of the null point P_3 is equivalent to setting the joint variable θ_3 to a particular value. Now, P_3 is translated along the \mathbf{z}_3 axis:

$$P_2 = T_{-d_3} P_3 \tilde{T}_{-d_3} \quad (101)$$

where T_{-d_3} is defined as in (27). Finally, we define the inner representation ℓ_2 of a line as in (43). The null point P_1 is found as the intersection point $\ell_1 \vee \ell_2$. Once the points P_0, P_1, P_2 and P_3 have been obtained, the joint variables d_1, d_2 and d_4 can be calculated as in equation (45).

6.3. $R+R+P+R$

The null point P_0 is translated along the joint axis \mathbf{z}_1 by an amount equal to the length of the first link, d_1 . Indeed, $P_1 = T_{d_1} P_0 \tilde{T}_{d_1}$, where T_{d_1} is defined as in (27). Now, the inner representation of a sphere is defined as:

$$s_1 = P_w - \frac{1}{2} d_4^2 e_\infty, \quad (102)$$

where d_4 corresponds to the length of the fourth link. To continue, an extra point is needed. Let us denote by P_3 the null point that satisfies:

$$P_3 \wedge S_1 = 0 \quad \text{and} \quad d(P_1, P_3) = d. \quad (103)$$

Since the second and third joint axes belong to the same plane, their links can be regarded as the sides of a triangle where, in addition, the third side is the line segment defined by P_1 and P_3 . As shown in section 5.1.3, the law of cosines can be applied in this situation to deduce the expression for the joint variable d_3 . The length of both sides, as well as the angle between the joint axes, are known: d_2 , d and α_3 . Therefore:

$$d^2 = d_2^2 + d_3^2 - 2d_2d_3 \cos(\alpha_3), \quad (104)$$

where, as explained in section 5.1.3, there are either two distinct positive solutions or a unique positive solution for d_3 . This proves the equivalence between the extra point P_3 and the joint variable d_3 , i.e., given a particular instance of d_3 , we use equation (104) to compute d and, with d , we define the null point P_3 as in (103). Finally, the null point P_2 is extracted from the intersection bivector defined by the following geometric objects:

$$\begin{aligned} s_2 &= P_1 - \frac{1}{2}d_2^2 e_\infty, \\ s_3 &= P_3 - \frac{1}{2}d_3^2 e_\infty, \\ \Pi_1 &= P_0 \wedge P_1 \wedge P_3 \wedge e_\infty. \end{aligned} \quad (105)$$

Once all the points have been obtained, it is easy to recover the joint variables θ_1 , θ_2 and θ_4 following the same steps as in sections 5.1.3 and 5.1.4.

6.4. $R+R+R+R$

As in the previous case, the null point P_1 is obtained as the translation of P_0 along z_1 . Thus, the points that remain to be found are P_2 and P_3 . Now, as stated in section 5.1.4, two spheres and one plane are required to calculate P_3 . One of such spheres is defined as in (102). For the other, we first consider a triangle whose sides are the second and third links. This triangle is similar to the one defined in the previous case: the side lengths are d_2 and d_3 , respectively, and the angle between both sides is α_3 . The law of cosines allows to compute easily the length d of the third side as:

$$d^2 = d_2^2 + d_3^2 - 2d_2d_3 \cos(\alpha_3), \quad (106)$$

where only the positive solution for d is taken. Now, the inner representation of the other sphere can be defined:

$$s_2 = P_1 - \frac{1}{2}d^2 e_\infty. \quad (107)$$

On the other hand, the outer representation of a plane, denoted by Π_1 , is computed as in (70). Clearly, P_3 can be extracted from the intersection bivector defined by these three geometric entities.

Once P_3 has been obtained, two new spheres should be defined to calculate P_2 . Their inner representations are:

$$\begin{aligned} s_3 &= P_1 - \frac{1}{2}d_2^2 e_\infty, \\ s_4 &= P_3 - \frac{1}{2}d_3^2 e_\infty. \end{aligned} \quad (108)$$

Again, the intersection of these two new spheres with the plane represented by Π_1 is computed as:

$$B = s_3 \vee s_4 \vee \pi_1, \quad (109)$$

where the null point P_2 is extracted from B . Finally, the joint variables $\theta_1, \theta_2, \theta_3$ and θ_4 are found in a similar way as in 5.1.4 by means of P_0, P_1, P_2, P_3 and P_w (with all their possible combinations).

7. Conclusions

This paper proposes a geometric strategy based on conformal geometric algebra for solving the inverse kinematics of serial robotic manipulators with 6 and 7 DoF and a spherical wrist. For manipulators of this kind, the inverse kinematics can be decoupled into two subproblems: the position and the orientation problems. The proposed approach solves the first subproblem by developing particular geometric strategies for each combination of prismatic and revolute joints that describe the position part of the robot. On the other hand, the second subproblem is solved by splitting the rotor that defines the target orientation of the end-effector into exactly three rotors, where each one of them depends on just one joint variable.

For non-redundant serial robots, this approach gives the entire set of solutions, while for redundant robots with 7 DoF, all the solutions are obtained as a one-parameter family of particular solutions where the parameter is one of the joint variables (the redundant joint). Therefore, we can consider the approach introduced here as a closed-form method. Moreover, since offsets between consecutive joints in the position part of the robot are also treated, we are solving the problem for simple and complex robot geometries. As reviewed in sections 1 and 2.1, closed-form methods are the most suitable for solving the inverse kinematics of serial robots. Since the most existing contributions of this kind are based either in the use of complex geometric formulations or matrix manipulations, the approach presented here becomes an elegant, efficient and intuitive alternative.

References

References

- [1] J. Denavit, R. S. Hartenberg, A kinematic notation for lower-pair mechanisms based on matrices, *Journal of Applied Mechanics* 22 (2) (1965) 215 – 221.

- [2] B. Siciliano, L. Sciavicco, L. Villani, G. Oriolo, *Robotics: Modelling, Planning and Control*, Springer Publishing Company, Incorporated, 2008.
- [3] M. Spong, S. Hutchinson, M. Vidyasagar, *Robot Modeling and Control*, John Wiley and Sons, 2006.
- [4] D. Pieper, *The kinematics of manipulation under computer control*, Ph.D. thesis, Stanford Artificial Intelligence Laboratory - Stanford University (1968).
- [5] A. Jikou Kouabon, A. Melingui, J. Mvogo Ahanda, O. Lakhal, V. Coelen, M. KOM, R. Merzouki, *A Learning Framework to inverse kinematics of high DOF redundant manipulators*, *Mechanism and Machine Theory* 153 (2020) 103978.
- [6] R. Paul, *Robot Manipulators: Mathematics, Programming and Control*, The MIT Press, 1981.
- [7] D. Jung, Y. Yoo, J. Koo, M. Song, S. Won, *A novel redundancy resolution method to avoid joint limits and obstacles on anthropomorphic manipulator*, in: *SICE Annual Conference*, Tokyo, Japan, 2011, pp. 924 – 929.
- [8] C. Yu, M. Jin, H. Liu, *An analytical solution for inverse kinematic of 7-DOF redundant manipulators with offset-wrist*, in: *IEEE International Conference on Mechatronics and Automation*, Chengdu, China, 2012, pp. 92–97.
- [9] L. Huang, R. Jiang, *A new method of inverse kinematics solution for industrial 7DoF robot*, in: *32nd Chinese Control Conference (CCC)*, Xi'an, China, 2013, pp. 6063 – 6065.
- [10] Y. Liu, D. Wang, J. Sun, L. Chang, C. Ma, Y. Ge, L. Gao, *Geometric approach for inverse kinematics analysis of 6-DOF serial robot*, in: *IEEE International Conference on Information and Automation*, Lijiang, China, 2015, pp. 852–855.
- [11] Y. Wei, S. Jian, S. He, Z. Wang, *General approach for inverse kinematics of nR robots*, *Mechanism and Machine Theory* 75 (2014) 97 – 106.
- [12] A. Aristidou, J. Lasenby, Y. Chrysanthou, A. Shamir, *Inverse kinematics techniques in computer graphics: A survey*, *Computer Graphics Forum* 37 (6) (2018) 35–58.
- [13] S. Buss, *Introduction to inverse kinematics with Jacobian transpose, pseudoinverse and Damped Least Squares methods.*, Tech. rep., University of California, San Diego (2009).
- [14] A. De Luca, G. Oriolo, *The reduced gradient method for solving redundancy in robot arms*, *RoboterSysteme* 7 (1991) 117 – 122.

- [15] H. Lau, L. Wai, A Jacobian-based redundant control strategy for 7DOF WAM, in: Proceedings Conference on Control, Automation, Robotics and Vision (ICARV), Singapore, 2002, pp. 1060 – 1065.
- [16] W. Wang, Y. Suga, H. Iwata, S. Sugano, Solve inverse kinematics through a new quadratic minimization technique, in: IEEE/ASME International Conference on Advanced Intelligent Mechatronics (AIM), Kachsiung, Taiwan, 2012, pp. 306 – 313.
- [17] C. Wampler, Manipulator inverse kinematic solutions based on vector formulations and damped least-squares methods, *IEEE Trans. Systems, Man, and Cybernetics* 16 (1) (1986) 93 – 101.
- [18] E. Bayro-Corrochano, D. Kähler, Kinematics of robot manipulators in the motor algebra, in: G. Sommer (Ed.), *Geometric Computing with Clifford Algebras: Theoretical Foundations and Applications in Computer Vision and Robotics*, Springer Berlin Heidelberg, Berlin, Heidelberg, 2001, pp. 471–488.
- [19] J. M. Selig, Robot kinematics and flags, in: E. Corrochano, G. Sobczyk (Eds.), *Geometric Algebra with Applications in Science and Engineering*, Birkhäuser Boston, Boston, MA, 2001, pp. 211–234.
- [20] A. Aristidou, J. Lasenby, FABRIK: A fast, iterative solver for the Inverse Kinematics problem, *Graphical Models* 73 (5) (2011) 243 – 260.
- [21] D. Hildenbrand, J. Zamora, E. Bayro-Corrochano, Inverse kinematics computation in computer graphics and robotics using conformal geometric algebra, *Advances in Applied Clifford Algebras* 18 (3) (2008) 699–713.
- [22] J. Hrdina, A. Návrát, P. Vašík, CGA-based robotic snake control, *Advances in Applied Clifford Algebras* 27 (1) (2017) 621 – 632.
- [23] J. S. Kim, J. H. Jeong, J. H. Park, Inverse kinematics and geometric singularity analysis of a 3-SPS/S redundant motion mechanism using conformal geometric algebra, *Mechanism and Machine Theory* 90 (2015) 23 – 36.
- [24] J. Zamora, E. Bayro-Corrochano, Inverse kinematics, fixation and grasping using conformal geometric algebra, in: *IEEE/RSJ International Conference on Intelligent Robots and Systems (IROS)*, Sendai, Japan, Vol. 4, 2004, pp. 3841–3846.
- [25] L. Campos-Macías, O. Carbajal-Espinosa, A. Loukianov, E. Bayro-Corrochano, Inverse kinematics for a 6-DOF walking humanoid robot leg, *Advances in Applied Clifford Algebras* 27 (1) (2017) 581–597.
- [26] S. Tørdal, G. Hovland, I. Tyapin, Efficient implementation of inverse kinematics on a 6-DOF industrial robot using conformal geometric algebra, *Advances in Applied Clifford Algebras* 27 (3) (2017) 2067–2082.

- [27] A. Kleppe, O. Egeland, Inverse Kinematics for Industrial Robots using Conformal Geometric Algebra, *Modeling, Identification and Control* 37 (1) (2016) 63–75.
- [28] C. Lavor, S. Xambó-Descamps, I. Zaplana, *A Geometric Algebra Invitation to Space-Time Physics, Robotics and Molecular Geometry*, SBMAC/SpringerBriefs, Springer, 2018.
- [29] H. Hadfield, L. Wei, J. Lasenby, The forward and inverse kinematics of a Delta robot, in: N. Magnenat-Thalmann, C. Stephanidis, E. Wu, D. Thalmann, B. Sheng, J. Kim, G. Papagiannakis, M. Gavrilova (Eds.), *Advances in Computer Graphics*, Springer International Publishing, 2020, pp. 447–458.
- [30] I. Zaplana, New perspectives on robotics with geometric calculus, in: D. A. X.-D. S (Eds.), *Systems, patterns and data engineering with geometric calculi*, ICIAM 2019 SEMA SIMAI Springer Series, 2021, pp. 1–17.
- [31] C. Doran, A. Lasenby, *Geometric Algebra for Physicists*, Cambridge University Press, 2003.
- [32] L. Dorst, D. Fontijne, S. Mann, *Geometric algebra for computer science: An object-oriented approach to geometry*, Morgan Kaufmann Publishers Inc., 2007.
- [33] A. Lasenby, J. Lasenby, R. Wareham, A covariant approach to geometry using geometric algebra, Tech. Rep. CUED/F-INFENG/TR-483, Department of Engineering - University of Cambridge (2004).
- [34] A. Aristidou, *Tracking and modelling motion for biomechanical analysis*, Ph.D. thesis, Department of Engineering - University of Cambridge (2010).
- [35] I. Zaplana, L. Basanez, A novel closed-form solution for the inverse kinematics of redundant manipulators through workspace analysis, *Mechanism and Machine Theory* 121 (2018) 829–843.